Materials and Design 195 (2020) 109062

Contents lists available at ScienceDirect

Materials and Design

journal homepage: www.elsevier.com/locate/matdes

Investigating the performance of 410, PH13-8Mo and 300M steels in a turning process with a focus on surface finish

Chris M. Taylor [a,*], Fernanda Díaz [b], Raúl Alegre [c], Thawhid Khan [d], Pedro Arrazola [c], James Griffin [e], Sam Turner [a]

[a] University of Sheffield AMRC, Wallis Way, South Yorkshire S60 5TZ, UK
[b] Manufacturing Department, Piso 4, 851 Beaucheff Puente, Santiago, Chile
[c] Faculty of Engineering, Mondragon University, Mondragon 20500, Spain
[d] Faculty of Science and Engineering, Manchester Metropolitan University, Chester Street, Manchester M15 6BH, UK
[e] Mechanical Automotive and Manufacturing, Coventry University, Priory Street, Coventry CV1 5FB, UK

HIGHLIGHTS

- Hardened engineering steels were investigated in finish turning. A turned surface roughness below 0.4 μm *Ra* could be consistently achieved.
- A method was developed to screen in a relatively simple way for more effective machining parameters.
- A generalised recommendation for good quality was a surface speed of at least 120 m/min and 0.088 mm/rev feed rate.

GRAPHICAL ABSTRACT

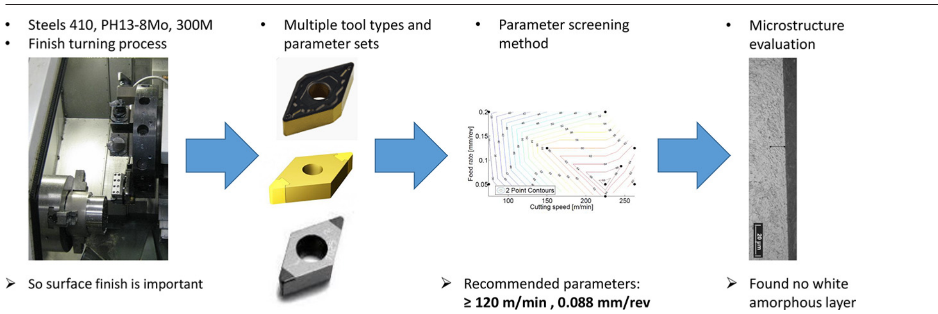

ARTICLE INFO

Article history:
Received 16 July 2020
Received in revised form 7 August 2020
Accepted 12 August 2020
Available online 15 August 2020

Keywords:
Hardened steels
Turning
Surface finish
Machinability

ABSTRACT

This study generated novel behavioural data for three engineering steels undergoing a turning process. The materials were hardened 410, PH13-8Mo and 300M, two stainless steels and one high strength steel respectively. A primary aim was obtaining low machined surface roughness. A surface finish investigation compared tool geometries and tool materials. Multi-response cutting parameter screening was undertaken using a novel trade study and iteration method, where the calculated cut quality was used to identify better feed rates and surface speeds. In addition the sub-surface machined microstructure was examined.

Tools with a small nose radius produced the roughest surfaces. A surface roughness below 0.4 μm *Ra* could be consistently achieved on all three materials using rhombic wiper inserts and a feed rate up to 0.1 mm/rev. PH13-8Mo had the lowest machined surface roughness, as low as 0.11 μm in terms of *Ra*. In the parameter screening stage a generalised recommendation for good cut quality was a surface speed of at least 120 m/min and a feed rate of 0.088 mm/rev. The microstructure examination showed that for all materials under the conditions tested, there was no evidence of white amorphous layer formation and there was grain deformation for the 410 material only.

1. Introduction

1.1. Review of current research

Authors such as [1–3] have defined stainless steels as difficult-to-cut materials. The principal factors that affect machinability were identified as the following: low thermal conductivity, tendency of high built-up

* Corresponding author.
E-mail addresses: c.m.taylor@sheffield.ac.uk (C.M. Taylor), ac0393@coventry.ac.uk (J. Griffin).

https://doi.org/10.1016/j.matdes.2020.109062

edge (BUE) formation even at high cutting speeds, high fracture toughness, a high level of work hardening and abrasive constituents.

Hard turning has the potential to replace cylindrical grinding processes, to achieve the required surface finish specification on appropriate hardened steel components. Hard turning by definition is applied to materials that have a hardness value above 45 HRC. An investigation completed by Matsumoto et al. [4] showed that hard turning had the capability to produce a relatively smooth surface finish. Advantages compared to grinding, such as higher material removal rates, lower cutting forces and the ability to machine complex parts with only one set-up, lead to lower costs when turning. In addition, with the possibility of dry cutting conditions a decrease in environmental impact ensures hard turning is an alternative to grinding for more sustainable manufacturing, as explored in [5,6]. Moreover hard turning creates benefits in terms of machined components' fatigue life, producing compressive residual stresses in the machining-affected near-surface layer [7] as opposed to tensile residual stresses. One feature which may arise is the near-surface phenomenon of amorphous white layer formation, although this can also occur when grinding [8]. Recent analyses of machined surfaces in the works [9–11] have measured roughness but also near-surface microstructure deformation and profiling of residual stress and micro-hardness. Xu et al. [10] tested the effect that these features had on the life of samples via fatigue testing.

Cutting parameters have an influence on surface roughness in machining. Investigations with examples being [12–14] have found that the feed rate is considered the most important parameter regarding surface finish. As a general rule, higher feed rates lead to higher roughness. However Dawson and Kurfess [15] observed that below a certain feed rate the tool repetitively rubbed the material as well as cutting it, which resulted in a worse surface quality. To summarise surface speed characteristics from investigations: experimental results from [16–18] indicated that surface roughness could be improved by increasing the surface speed parameter with an optimal operating window; work by Korkut et al. [2] attributed this relationship to the presence of BUE at lower surface speeds; furthermore Tekiner and Yeşilyurt [3] found that the height of the BUE decreased as the surface speed increased.

The use of specific tooling has an important effect on surface finish. Chou and Song [19] explained that the resulting surface finish improved with a large tool nose radius. In terms of tool geometry, improvement has been seen when using technologies such as the wiper tool insert, which takes advantage of having multiple nose radii. Grzesik and Wanat [20] recommended the use of tools with wiper geometry for obtaining the same or even better surface finish when compared with standard insert geometries, even when applying double the feed rate.

The type of cutting tool substrate and coating is also important, determining the type and degree of tool-workpiece chemical interactions such as adhesion and diffusion [21]. For this reason the following study involved three different insert substrates.

1.2. Objectives for study

A primary aim of this work was to obtain a high quality turned surface finish and demonstrate that a surface roughness could be achieved which was within the typical range obtained for finish grinding processes. Relatively little experimental machinability data was available for turning of the three alloys of interest which were 410, PH13-8Mo and 300M so characterisation activity was a priority. In addition to this, a more effective method to screen different machining configurations (such as the tool geometry, tool materials and cutting parameters) was required in order to iterate towards a higher-quality process output. With that in mind, the study's objectives were to:

- Test tool inserts of various geometries and material grades, regarding the resulting surface finish;
- Develop an enhanced method to investigate the relationship between turning input parameters and the quality of the resulting cut, with the quality being a calculated function of the machinability metrics surface roughness, productivity, tool wear, cutting forces and chip morphology;
- Establish suitable parameters for finish turning to achieve the desired cut quality for the three steel types;
- Examine the effect of machining on the near-surface microstructure, including grain deformation and the potential for amorphous white layer formation.

To determine the influence of the cutting insert type on surface finish, the initial experimental activity investigated multiple aspects of tool configuration and workpiece materials in a wider sense. The number of process inputs being varied reduced as the trials activities progressed.

2. Experimental set-up, methods and data processing

Turning experiments were carried out on a MAG Hawk 300 CNC lathe as displayed in Fig. 1, with a 37 kW motor providing a maximum spindle speed of 3000 rpm. The work materials machined were the following. 300M, also known as S155, is a high strength form of AISI 4340 low alloy steel, generally considered a difficult to cut material because of its toughness and strength. 410 is a martensitic quench-hardenable stainless steel and PH13-8Mo is a martensitic precipitation-hardenable stainless steel. The three steels are commonly used in aerospace components as well as in bolts, in fasteners and for other demanding applications. 300M is the least corrosion-resistant of the steels. 300M, 410 and PH13-8Mo steels are as per the specifications ASTM A579 (32), ASTM A276 and ASTM A564 XM13 respectively. All three steels were pre-processed with hardening heat treatments. Table 1 displays the materials' heat treatment and measured hardness.

A summary of fixed and variable experimental parameters appears in Table 2 for ease of reference. The radial depth of cut was fixed at 0.25 mm for all trials, which is typical of a finish turning operation after heat treatment. A new insert edge was used for each cut. There were hundreds of potential insert combinations which could be selected for this turning application, so the tooling supplier was consulted to aid in the selection of a variety of suitable options to test. For more details on how to select a turning insert for a specific application the following guide can be consulted [22].

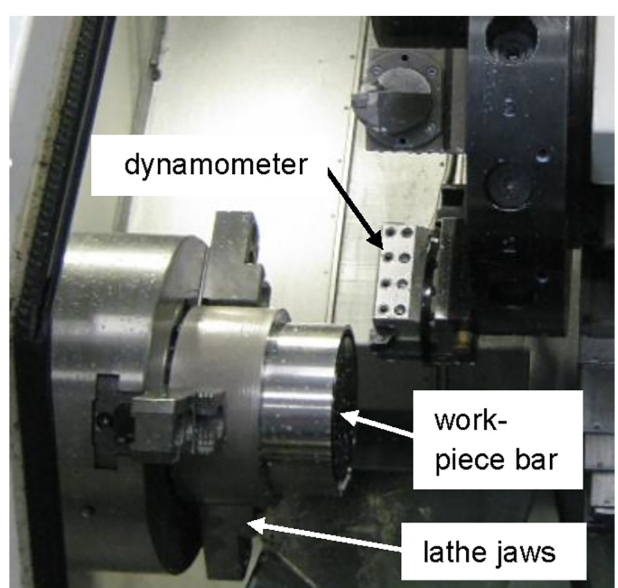

Fig. 1. Lathe set-up for turning trials.

Table 1
Materials' heat treatment and hardness. Material supplier, Tata Steel.

Alloy name	Heat treatment	Hardness (HRC)
410	Harden and temper	40.9
PH13-8Mo	Solution treat, subzero treat and H950 age	48.9
S155 (300M)	Harden and temper	54.7

The following inserts with various substrate materials and geometries were used, these were selected based on comparable historical performance data and conversations with the tool supplier. Two tungsten carbide/ cobalt inserts were used: DNMG 150604-PM 4215 with tool nose radius of 0.4 mm and DNMX 150616-WMX 4215 with tool nose radius of 1.6 mm and wiper geometry. Three cubic boron nitride (CBN) inserts were also entered into surface finish testing: DNGA 150416EA 7015 with nose radius 1.6 mm, DNGA 150404-S01030A 7015 with nose radius 0.4 mm and DNGA 150412-S01030AWH 7015 with a wiper and nose radius 1.2 mm. Finally, one cermet insert was tested, DNMX 150608-WF 1525 with a wiper and tool nose radius 0.8 mm.

The cutting tool grade details are as follows: GC4215 has a substrate based on tungsten carbide with a spatial gradient of grain size, covered with a thick chemical vapour deposited (CVD) coating consisting of combined titanium carbonitride and nitride plus aluminium oxide. CB7015 has a CBN substrate with a thin physical vapour deposited (PVD) coating consisting of titanium nitride. GC1525 has a cermet substrate with a thin PVD coating consisting of titanium carbonitride and nitride. Carbide-based inserts of the type used in this study have a cutting edge hone radius in the region of 30 μm. Edge hones are applied to cutting inserts by the manufacturers prior to coating application, using methods such as brushing and grit blasting. To benchmark the repeatability of cutting edge honing, from a population of 25 coated tungsten carbide cutting inserts 100 cutting edges were measured using an Alicona SL non-contact high-resolution 3D microscope with EdgeMaster software to obtain edge radius measurements. The standard deviation for the cutting edge radius was found to be 9.4% of the mean edge radius value. In terms of CBN geometries, CBN tools with 'S01030' geometry have an S-type land on the cutting edge, which is 0.1 mm wide with 30 degrees of chamfer and features a honed cutting edge. The S land provides additional edge strength. 'EA' type edge geometry indicates an E land, which features the edge hone but no chamfer. A typical hone radius for these lands is around 15 μm.

All inserts were mounted in a shank-style toolholder which was bolted into a dynamometer. The lathe delivered a directed flood of 6% concentrated Houghton Hocut 795B coolant through a nozzle in the toolholder body to the insert position, at 14 l/min flowrate. A Kistler 9121 turning dynamometer and an acquisition system were used to hold the turning toolholder and to collect the cutting forces. The acquisition system included a charge amplifier and Dynoware software. From the acquired force data, results were extracted where the forces repeated in a stable manner against time. Force data was averaged over a time period which equated to ten revolutions of the turned bar.

Table 2
Fixed and variable experimental parameters. For more details of configuration see section 2 text.

Fixed parameters	Variable parameters
Machining process type- outer diameter turning. Radial depth of cut- 0.25 mm. Axial length of cut- 12 mm. Tooling supplier- Sandvik Coromant. Turning insert shape- D. Insert size- 15 mm. Tool holding and cutting fluid application held constant. Insert type tested in later parameter screening and microstructure analysis trials- DNMX 150616-WMX 4215.	Three steels- 410, PH13-8Mo, 300M. Surface speed- from 30 to 330 m/min. Feed rate- from 0.005 to 0.2 mm/rev. Various cutting tool edge geometries and grades tested in surface finish testing (first stage of trials).

Potential dynamics effects were mitigated to ensure that the measured surface profile was not unduly affected by any vibration marks. Mitigations were: (1) configuring a stiff workpiece structure, i.e. which was relatively short in length and large in diameter; (2) minimising protrusion of the tool holder from its clamping arrangement; (3) cutting with a small depth of cut to produce relatively low cutting forces; and (4) checking that vibrations were not audible during cutting or visible on the cut surface after cutting.

The machined surface roughness was measured with a Mitutoyo SJ-301 device. To position the turned bar and roughness measurement stylus relative to each other in a stable fashion, the bar was removed from the lathe and mounted on V-blocks. The stylus was held in a clamp stand, as Fig. 2 displays. All surface roughness measurements were taken six times around the bar's circumference, then averaged. Wear occurring near the cutting edge of the turning inserts was captured and measured using a Carl Zeiss Stemi 2000 desktop microscope and associated software. For photographs of similar hardware to that used for measuring surface roughness and tool flank wear, see the paper [23].

Surface roughness tests during trials stage 1 were carried out based on three feed rates: 0.05, 0.1 and 0.2 mm/rev. Each cutting pass consisted of 4 mm axial length to reach steady cutting conditions, then a further 8 mm of steady state cutting for data collection. The total axial length of cut was 12 mm. The bar diameters varied between 130 and 70 mm during cutting. Each cutting pass comprised between 60 and 2400 spindle revolutions and the resulting spiral cut length per pass was between 20 and 800 m.

In this stage of trials the six insert types were tested on the steel PH13-8Mo, chosen because it has an intermediate hardness considering the three steels tested. The best overall insert and the best carbide insert with regard to surface finish were then tested on the other two steels. Additionally, on PH13-8Mo three low feed rates were tested: 0.005, 0.01 and 0.025 mm/rev, using the best down-selected carbide insert and the same methodology.

Machining processes are complex, having many significant and interdependent inputs and outputs [24]. When a factor such as the feed rate or surface speed changes, multiple process responses change simultaneously with examples being the machined surface finish, cutting forces, tool wear rates, chip formation and productivity (machining rate). When configuring a process it is desirable for manufacturing engineers to be able to methodically iterate towards machining parameters which provide better combinations of these process responses. With that in mind a novel parameter screening method has been devised.

A trade study method was developed to evaluate then combine the relevant process outputs into a single cutting quality metric (score) which was then mapped against cutting parameters. Contour maps

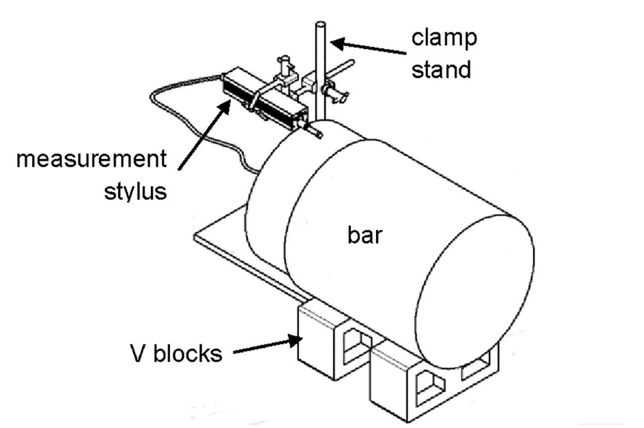

Fig. 2. Roughness measurement set-up.

indicate trends in the cut quality allowing for iteration of the cutting parameters. The goal is to move in the direction of increasing cut quality to find the maximum score obtainable. The screening of cutting parameters for a combination of cutting tool and workpiece material is inspired by the AFNOR machinability standard [25]. The use of a trade study and mapping of the scores are new additions.

To engage effectively with this method it is necessary to understand the relative importance of the process responses and the trade-offs which can be made, which is typically within the remit and skill set of manufacturing engineers. The method has been designed to be accessible to and understandable by a wide potential group of end users. It has been implemented in MATLAB but could be transferred to other mathematical software.

To test this screening methodology the second stage of trials was parameter screening, conducted on all three steels with a combination of feed rates and surface speeds. Data regarding surface roughness, material removal rate, cutting forces, insert wear condition and the morphology of cut metal chips (sometimes known as swarf) were all evaluated and entered into a trade study system. In the case of roughness and forces a low value is good, so output scores were reciprocals to give a high cut quality where roughness and forces were low. The trade study output scores were used to construct cut quality (machinability) contour maps. The maps were created using MATLAB software and are displayed below. A scheme as follows was designed to evaluate cut quality across different materials, feeds and speeds and iterate towards the conditions for better machinability. Firstly five cuts were taken in material PH13-8Mo. The initial cutting parameters were a combination between three feed rates: 0.05, 0.1 and 0.2 mm/rev and three surface speeds. Surface speeds selected were based on the value *V15*, which was the surface speed estimated by the tool supplier where the cutting edge would last for 15 min before becoming excessively worn. A speed below *V15* should lead to a tool life beyond 15 min, whilst cutting faster than *V15* would be expected to cause more rapid tool wear and a life of less than 15 min. The surface speeds selected were the estimated *V15*, then half of *V15*, and 1.5 times *V15* (as per Fig. 3). Initially-estimated *V15* values for PH13-8Mo, 410 and 300M were 150, 180 and 60 m/min respectively. Then by evaluating the trade study score for these feed and speed combinations as described below it was possible to see the trend in cut quality, and four more parameter points were added in the region of the best results to find better cutting conditions for PH13-8Mo. For the other two steels a leaner screening method was used. Just three parameter points were tested at the beginning: the two extremes in surface speed were tested in combination with the high, low and medium feed rates.

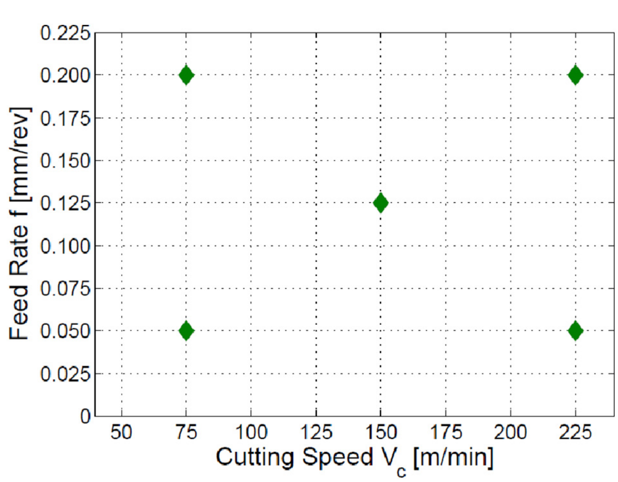

Fig. 3. Initial parameter combinations in material PH13-8Mo.

Table 3
Evaluation of five output scores in the second testing stage (parameter screening). Subscripts: '*S*' refers to smallest value measured, '*H*' refers to highest value measured, '*C*' is current measured value.

Output parameter	Quantity being scored	Output scoring evaluation
Surface roughness, *SR*	Average roughness *Ra*, using roughness tester	$10. Ra_S / Ra_C$
Productivity, *PR*	Productivity, expressed through material removal rate, *MRR*	$10. MRR_C / MRR_H$
Tool wear, *TW*	Insert degradation, inspected by microscope	1 (worn out) to 10 (as new condition)
Cutting forces, *CF*	Resultant time-averaged cutting force, *F*	$10. F_S / F_C$
Chip morphology, *CM*	Chip length, curling and tangling by visual inspection	1 (continuous uncontrolled, tangled chip) to 10 (short chip with limited curl)

The five output metrics evaluated in these screening trials are as indicated in Table 3, these metrics were all scores in the range from 0 to 10. The output parameters *TW* and *CM* as described in Table 3 were evaluated by comparison against a full spectrum of reference images of worn cutting edges and chips collected.

The material removal rate *MRR* (in cm^3/min) was calculated as per Eq. (1) and the dimensionless cut quality indicator *CQ* was calculated from the output scores via trade study style weightings as per Eq. (2).

$$MRR = V_c.a_p.f \tag{1}$$

$$CQ = 4.SR + 2.PR + 2.TW + 1.CF + 1.CM \tag{2}$$

V_c is the surface speed in m/min, a_p is the depth of cut in mm and f is the feed per revolution in mm. The parameters in Eq. (2) are as defined in Table 3.

On examination of Eq. (2) a reasonable question to ask would be how the weighting coefficients were determined. For instance, in the case of a rough machining process the role of surface finish would be less important. For a highly-automated process it might be more important to have consistently small chips which could be easily cleared without human intervention. The end user who is the expert, such as a manufacturing engineer or technician, is expected to decide the relative importance of the process responses in determining the overall cut quality. In the case of this work the end users wished to replace a grinding process with a turning process. Thus when the end users were consulted their requirements placed high importance on the surface finish *SR*, with a high weighting of 4 for that output metric. The end users similarly used their experience to determine the other four weightings. These weightings could be adjusted for a different case study to place a different relative importance on the responses considered, or indeed to consider other responses. If all five responses were evaluated and scored at 10, irrespective of the weightings applied the maximum cut quality score *CQ* of 100 would be the result.

A trade study is not the only means available for combining multiple responses to find the 'best' available result. Methods for multi-objective optimisation [26] were considered. Successive Pareto optimisation and genetic algorithms are two examples of potential methods to use. The two main reasons for selecting a trade study approach over more sophisticated methods were that a method was preferred which could be simply understood by a wide potential group of end users, also that developing more complex optimisation methods was not within the time scope of the work undertaken. Trade studies are a commonly-utilised method of assessment, examples can be found in other recent machining research works [27].

After the parameter screening exercise the best cutting parameters identified were then used in the third testing stage to generate cut surface samples for examination. After machining, cross-sectional surface samples were extracted by wire electrode discharge machining (wire EDM). These samples were then mounted, polished, etched and microscopically examined with a Leica optical microscope to determine the effect of machining on the near-surface microstructure.

3. Results and discussion

3.1. Surface roughness screening

Fig. 4 displays the results with respect to different feed rates, for the inserts tested in the stage 1 surface roughness trials.

A significant difference in the results can be observed based on the feed rates applied. In most cases a low feed rate (0.05 mm/rev) leads to a superior surface finish with mean roughness (*Ra*) values as low as 0.13 μm.

The influence of the insert geometry can also be discerned. Inserts with the smallest tool nose radius (0.4 mm, insert types 1 and 4 in Fig. 4) obtained the most variable results with regard to feed rate, obtaining *Ra* values higher than 2 μm at 0.2 mm/rev. This occurred in the cases of both carbide and CBN inserts. Wiper inserts demonstrated a better performance than the standard tool nose inserts. This is demonstrated in Fig. 4 where the roughest three cases (tool types 1, 3 and 4) involve standard tool nose radii. The underperformance of standard inserts is more significant at high feed rates.

With the CBN 1.2 mm nose wiper insert tool 5, the lowest roughness value obtained was 0.13 μm but the associated result for the highest feed rate was not so good, being close to the stipulated 0.4 μm roughness limit. The best overall result was achieved by the wiper cermet insert tool 6. Of the carbide-based options, the 1.6 mm nose wiper insert tool 2 was considered best because of its good performance at both low and high feed rates, performing almost as well as tool 6. Tungsten carbide is the most popular and affordable insert type, hence both the carbide and cermet DNMX inserts (tools 2 and 6) were tested for surface finish on all three steel types.

Fig. 5 displays the results of finish turning with two insert styles on all three steels. Analysing the results it can be deduced that feed rates of 0.05 and 0.1 mm/rev constantly achieved a surface finish *Ra* below the target level of 0.4 μm. The typical surface roughness range for grinding processes is from 0.1 to 1.6 μm [28] so the turning configurations studied are falling within the lower half of that typical range. Only 300M had turned surfaces rougher than the target value, at the high feed rate 0.2 mm/rev. In terms of insert selection, Fig. 5 shows that sometimes the cermet insert designated as ‘2’ outperformed the carbide tool designated as ‘1’, and vice versa. Purely on the basis of nose geometry and taking prior findings into account as per section 1.1, a larger insert nose would be expected to produce lower surface roughness. Based on Fig. 5 this was not consistently the case, particularly for PH13-8Mo. However tungsten carbide inserts showed much better wear resistance than cermet in a parallel study, which will be reported in a separate publication. Thus the carbide insert design DNMX 150616-WMX 4215 was used in all further testing reported below.

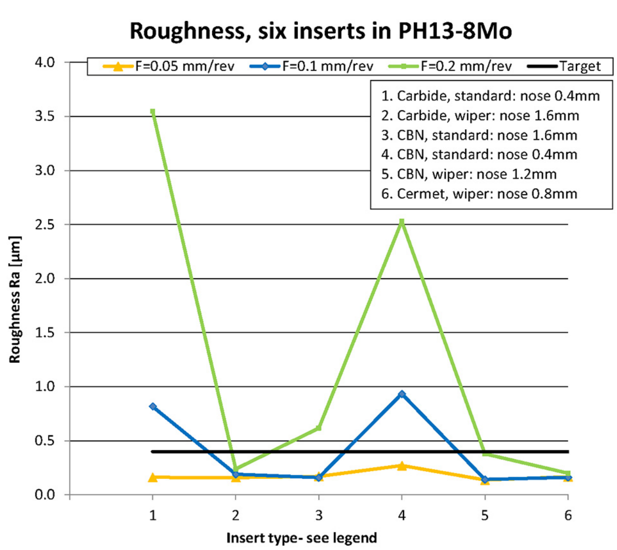

Fig. 4. Roughness *Ra* for six different inserts at three feed rates on PH13-8Mo steel. Surface speed 150 m/min for inserts 1 and 2, 230 m/min for inserts 3, 4 and 5 and 180 m/min for insert 6. Speeds recommended by tool manufacturer.

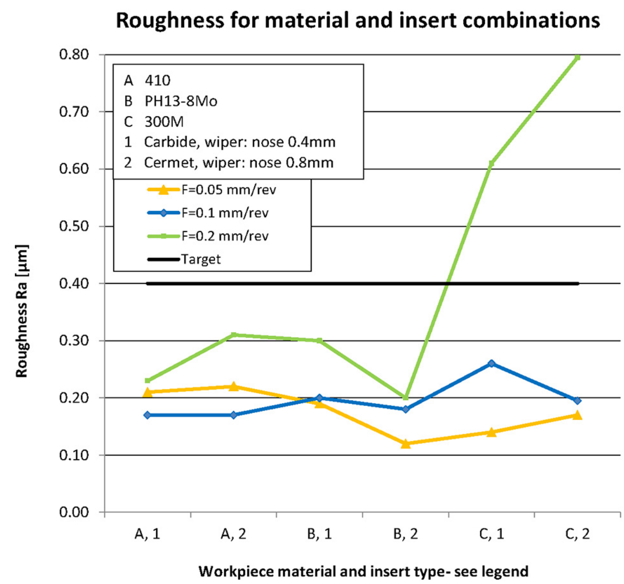

Fig. 5. Roughness for best carbide and cermet inserts, on the three steel materials. Surface speed 180 m/min.

3.2. Low feed rates

As seen in the work reviewed above [15], below a certain feed rate value the surface finish produced starts to worsen. Results in Fig. 6 also show this tendency, where an optimum value of 0.025 mm/rev provides the lowest surface roughness. At lower feed rates, the insert rubs repeatedly against the workpiece, work hardening it instead of cutting it. Fortunately it is not desirable to cut at such slow feed rates because of the productivity disadvantages. The feed rate value corresponding to the minimum measured roughness is related to the cutting edge hone radius of the insert tested- for higher feed rates more cutting

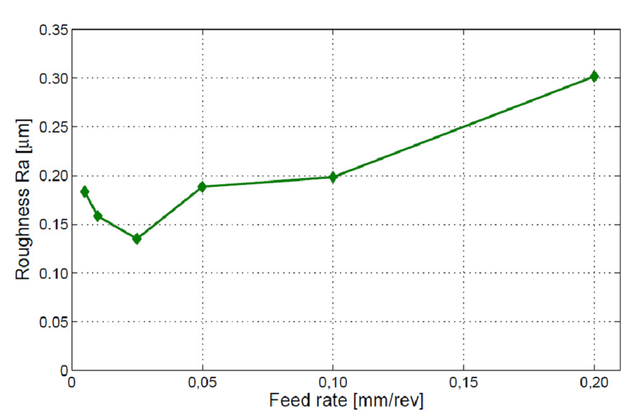

Fig. 6. Roughness at low feed rate. Material PH13-8Mo, surface speed 180 m/min.

Fig. 7. Cut chips from trials. (a) overall best case, 300M. (b) worst case, 410.

(shearing) occurs with less rubbing. Feed rates for the work to follow feature a lower limit of 0.025 mm/rev for this reason. Considering the results exhibited in section 3.1 and considering that the target for turned roughness was 0.4 μm, a maximum feed rate of 0.2 mm/rev was selected.

3.3. Parameter screening

Example outputs from the parameter screening trials can be viewed in Fig. 7 and Fig. 8. Fig. 7a shows the overall highest-scoring turned chips collected, for material 300M and using the parameter set 120 m/min and 0.0875 mm/rev. These chips were relatively short and untangled which would facilitate easy removal with minimal disruption to the process. Fig. 7b shows the opposite, the overall lowest-scoring chips collected for 410 and using the parameter set 90 m/min and 0.125 mm/rev.

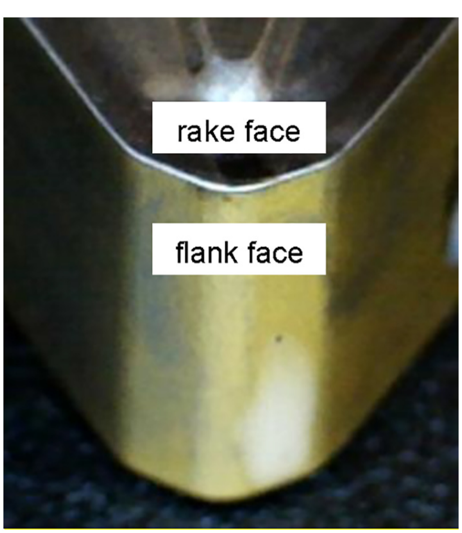

Fig. 8. Example tool condition image showing minimal damage after cutting.

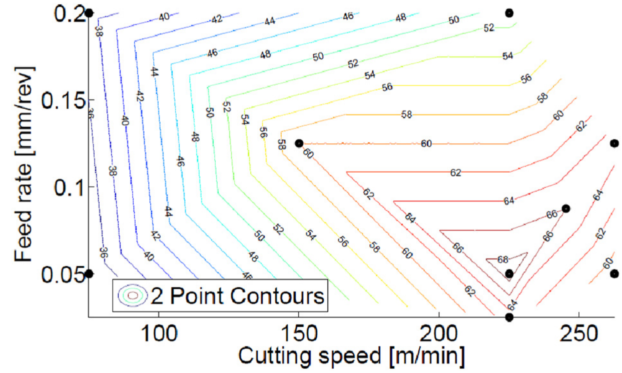

Fig. 9. Contour map of overall cut quality (*CQ*) scores for material PH13-8Mo.

These chips were described as long, curled and tangling around the bar during cutting. Next, shown in Fig. 8 is an example of a cutting edge after use. Each cutting edge was examined for the severity of damage features to generate a tool condition score. In the example shown the insert had relatively little damage but there was evidence of workpiece adhesion (the shiny material) on the cutting edge line and a small amount of tool material removed on the flank just below the cutting edge line. Results such as these were converted into numerical form by scoring each case out of 10.

After obtaining weighted output scores as per Eq. (2) from the initial parameter testing cuts, further parameter combinations were analysed, moving towards better cut quality scores in a quick and iterative fashion. Contour maps graphically illustrated the trend in cut quality against feed and speed for the given workpiece materials. The variables *CQ*, *SR* and *CF* are plotted in the contour graphs displayed. Refer to Table 3, Eq. (1) and Eq. (2) for the definition of these three variables. Please refer to section 2 for more explanation of how and why the contour graphs were constructed.

In the case of material PH13-8Mo, Fig. 9 displays the cut quality (*CQ*) related scores and it is possible to see the best score achieved, which is at 225 m/min surface speed and 0.05 mm/rev feed rate. The productivity component of the cut quality score has not been plotted- it would simply increase towards the top right of the contour map, i.e. increasing with feed and speed.

The most test results were obtained for PH13-8Mo material so the trends in terms of roughness and forces can be seen well. Fig. 10 displays the PH13-8Mo roughness scores. It is possible to observe a tendency which has been reported in prior literature: roughness generally decreases with reducing feed rates and higher surface speed. Roughness values in the bottom right quadrant of the contour map are the lowest, between 0.11 and 0.15 μm in terms of *Ra*. Low roughness leads to high

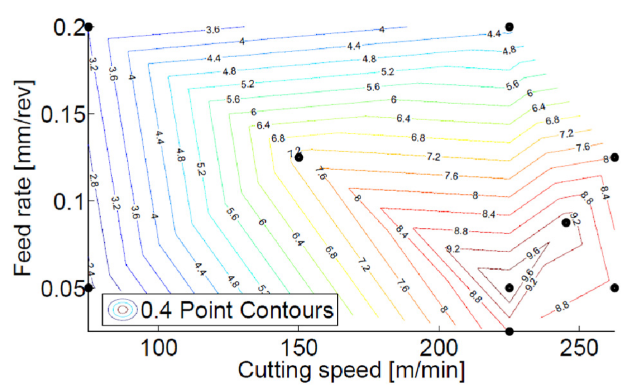

Fig. 10. Contour map, reciprocal machined roughness (*SR*) scores for PH13-8Mo.

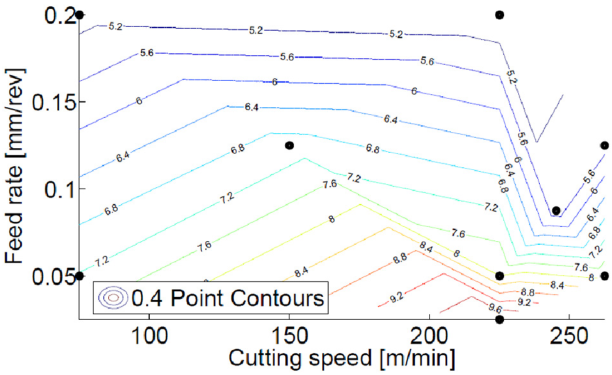

Fig. 11. Contour map, reciprocal cutting force (*CF*) scores for PH13-8Mo.

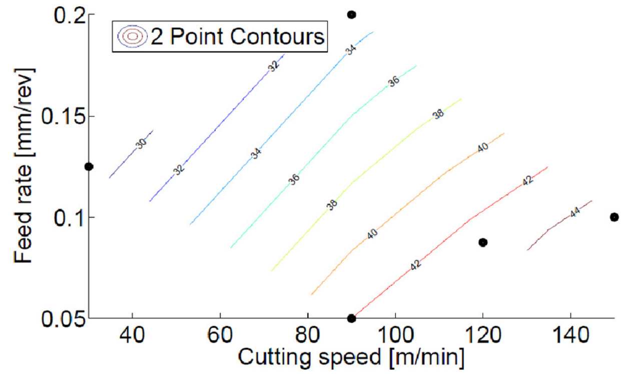

Fig. 13. Contour map with overall cut quality (*CQ*) scores for material 300M.

corresponding *SR* scores, calculated at between 7.4 and the maximum possible of 10. By increasing the feed rate to 0.2 mm/rev, the roughness increased to 0.27 μm. The worst case scenario was 0.5 μm average roughness with a calculated *SR* score of 2.3, at the lowest surface speed and feed rate (75 m/min and 0.05 mm/rev).

Fig. 11 displays the PH13-8Mo cutting force scoring map. The pattern is not the same as for Fig. 10, partly because the cutting force drops monotonically with feed rate. The maximum force was recorded at high and low speed for 0.2 mm/rev, resulting in 356 and 370 N recorded respectively. These forces correspond to calculated *CF* values of 5.0 and 4.9. The minimum force value was 180 N at 225 m/min and 0.025 mm/rev, which corresponds to the maximum *CF* score of 10.

For the 410 stainless steel the same style of contour maps were obtained. Lower scores were obtained with this material compared to PH13-8Mo. Fig. 12 illustrates the contour map for the cut quality of the 410 material. Compared to the PH13-8Mo the increase in surface speed also improved the cut quality, but in this case the optimum feed rate had a higher value. The obtained surface finish was worse than in PH13-8Mo, so lower roughness scores were obtained. The surface finish worsened at the highest speed and feed rate and also at the lowest surface speeds.

Consistent with Fig. 7, out of the three materials 410 showed the overall worst chip morphology and breakability. Referring to Annex G of the standard ISO 3685 [29], chips most resembled 'type 2.3', being snarled and tubular. The obtained chip was unbroken and in most cases tangled around the bar and tool, rubbing against the surface and damaging the tool. Without mitigation measures, such chips would be expected to lead to a scratched machined surface and poor prospects for process automation.

The cut quality scores obtained for material 300M were lower than those obtained for the 410 and PH13-8Mo materials. The contours in Fig. 13 increase towards the bottom right edge of the tested region, showing that the peak cut quality was not found for this trial which suggests that higher speeds should be tried. The tendency for the cut quality trend in Fig. 13 is the same as the one for the PH13-8Mo material, increasing the score by increasing surface speed. The surface finish values were inferior compared with the other two materials, obtaining the worst surface quality when machining at high feed rates. It was also noted that chip control worsened at high feed rates.

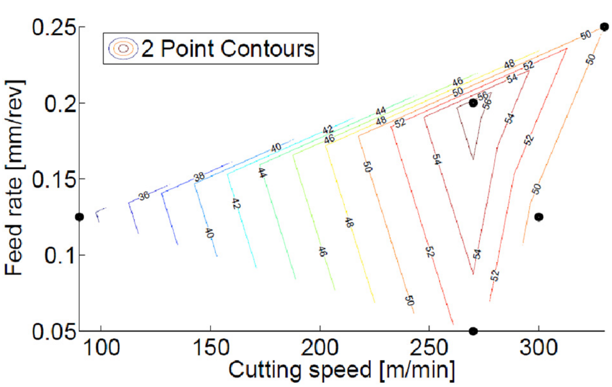

Fig. 12. Contour map with overall cut quality (*CQ*) scores for material 410.

Considering the results presented, it can be seen that high surface speeds gave a better surface finish, lower cutting forces, better chip breaking and also better productivity. The quality of cut generally increased with surface speed, in the ranges tested.

The feed rate produced a relatively small variation in surface roughness below 0.1 mm/rev. Above 0.1 mm/rev much higher surface roughness resulted. However if low cutting forces are a requirement, low feed rates are the best option. Generally the feed rate had more influence on the measured forces than the surface speed. There was no clear trend between feed rate, chip morphology and chip breakability. The low level of tool wear encountered in screening trials did not have any marked effect on surface roughness, instead the effect of cutting parameters on feed marks (cusps) combined with metallurgical-chemical interactions such as adhesion [30] are thought to have been more prevalent. If the inserts were run for longer periods of time it is expected that the measured roughness would gradually increase due to tool wear effects.

General recommendations for finish turning the three materials (with radial depth of cut 0.25 mm) would be to use surface speeds of at least 120 m/min. Examining all results, a feed rate of 0.088 mm/rev was determined as suitable to be used on all three materials.

This method of calculating a cut quality score then contour mapping that score against turning parameters permits identification of the trends in cut quality, further permitting the parameters to be adjusted to improve the output. The method requires that only a few tests be performed with a small amount of steel material consumed. Alternative methods for parameter screening, data modelling for prediction [31], extrapolation and optimization exist [32], these are also worthy of consideration.

3.4. Machined near-surface microstructure

The carbide DNMX 4215 insert type was used to turn finished surfaces for microstructure examination. Via parameter screening the feed rate used was 0.088 mm/rev. *V15* life tests (to be reported in future work) identified suitable material-specific surface speeds of 305, 395 and 195 m/min for PH13-8Mo, 410 and 300M materials respectively. Surfaces were turned for each material using these parameters. Surface samples were extracted and prepared then micrographs were created, as described in section 2. Micrographs were checked for near-surface features, specifically grain deformation and the formation of an

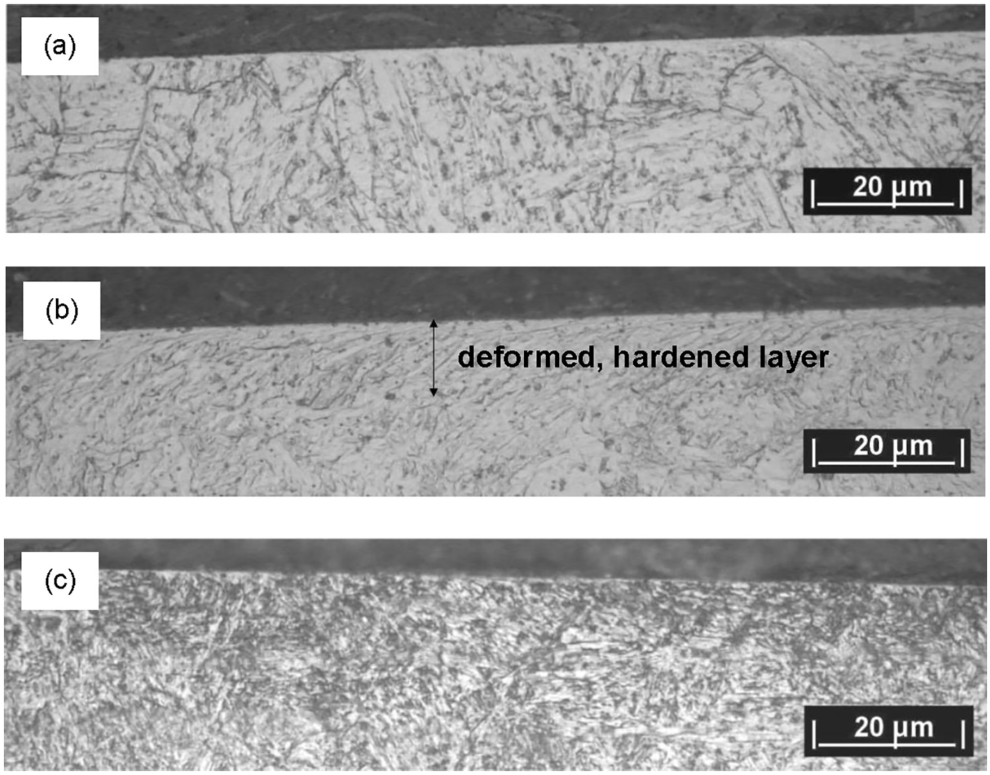

Fig. 14. Near-surface microstructure images for turned materials: (a) PH13-8Mo, (b) 410 and (c) 300M.

amorphous white layer. A white layer is a hardened surface layer [33] which has undergone a thermally and mechanically induced transformation, as such it is resistant to etching and appears white when inspected with a microscope. White layers are considered to be a risk-raising microstructure feature because they are hard and brittle [34]. They are susceptible to crack initiation which can reduce the fatigue life of engineering components in service [35].

Only material 410 showed evidence of work hardening and grain deformation on the surface, up to a depth of 10 to 15 μm as indicated in Fig. 14b. It is considered as a cold-worked layer formed during turning. PH13-8Mo and 300M (Fig. 14 parts a and c respectively) showed no evidence of a deformed sub-surface layer. There was no evidence of any white layer formation for all three turned material samples.

4. Conclusions

In this study three hardened engineering steel materials were finish turned with 0.25 mm radial depth of cut, in three stages. The stages were: firstly surface finish evaluation, secondly parameter screening and thirdly, sub-surface microstructure examination. The following conclusions can be made.

1. The steel PH13-8Mo machined with the lowest resulting surface roughness, which was as low as 0.11 μm in terms of *Ra*. The steel 410 was second best in this respect, with 300M steel creating the roughest surfaces. In terms of insert geometry, tools with a small nose radius produced the roughest surfaces, particularly at high feed rates. Tools with large nose radii created a smoother finish but wiper geometries performed better, controlling roughness well at the feed rate 0.2 mm/rev. A surface roughness below 0.4 μm *Ra*, which is within the range typically associated with grinding processes, could be consistently achieved on all three materials when using rhombic wiper inserts and a feed rate up to 0.1 mm/rev.
2. The multi-response parameter screening exercise yielded the generalised parameter recommendation of at least 120 m/min surface speed and a 0.088 mm/rev feed rate. The material removal rate and cutting forces increased monotonically with feed rate. However, surface roughness improved then worsened during trials where the feed rate was increased from 0.005 to 0.2 mm/rev, with a minimum roughness value at 0.025 mm/rev. The effect of feed rate on tool wear and chip breaking was indeterminate from the tests done. The 410 steel displayed the worst chip breaking behaviour resulting in long, uncontrolled tangling chips during finish turning.
3. Microscopic examination of the turned near-surface region revealed 10 to 15 μm depth of grain deformation in the 410 material, and no deformation effects in the other two materials. None of the three materials showed evidence of white amorphous layer formation under the conditions tested, which involved speeds in excess of 190 m/min.

Recommendations for future work include parameter screening at higher surface speeds on the material 300M due to indications that this would improve the cut quality. Full tool life testing activity compliments the work reported here, tool wear tests will be reported on in future work. Finally, for the surfaces which underwent microstructure analysis it would be beneficial to measure sub-surface residual stresses also, for a fuller picture of the interaction between the materials and the turning process.

Credit author contribution statement

Chris M Taylor: conceptualization, supervision, methodology, formal analysis, writing – original draft, writing - editing and reviewing **Fernanda Díaz**: investigation, formal analysis, writing – original draft, writing - editing and reviewing **Raúl Alegre**: investigation, validation **Thawhid Khan**: writing – editing and reviewing **Pedro Arrazola**: supervision, resources **James Griffin**: supervision, resources **Sam Turner**: conceptualization, funding acquisition, resources.

Role of the funding source

This work was funded by Tata Steel UK, who were not involved in the carrying out of the work.

Data availability

The raw and processed data required to reproduce these findings cannot be shared at this time as the data also forms part of an ongoing study.

Declaration of Competing Interest

The authors declare that they have no known competing financial interests or personal relationships which might influence the impartiality of the information in this paper.

Acknowledgements

The authors wish to thank Tata Steel UK and the University of Chile for supporting this work. Thank you to Johan Blachon for his help and advice during the trials.

References

[1] J. Paro, H. Hänninen, V. Kauppinen, Tool wear and machinability of X5 CrMnN 18 18 stainless steels, J. Mater. Process. Technol. 199 (2001) 14–20.
[2] I. Korkut, M. Kasap, I. Ciftci, U. Seker, Determination of optimum cutting parameters during machining of AISI 304 austenitic stainless steel, Mater. Des. 25 (2004) 303–305.
[3] Z. Tekiner, S. Yeşilyurt, Investigation of the cutting parameters depending on process sound during turning of AISI 304 austenitic stainless steel, Mater. Des. 25 (2004) 507–513.
[4] Y. Matsumoto, C.R. Liu, M.M. Barash, Residual stress in the machined surface of hardened steel, High Speed Mach. (1984) 193–204.
[5] A. Sahoo, B. Sahoo, Experimental investigations on machinability aspects in finish hard turning of AISI 4340 steel using uncoated and multilayer coated carbide inserts, Measurement 45 (2012) 2135–2165.
[6] R. Pavel, I. Marinescu, M. Deis, J. Pillar, Effect of tool wear on surface finish for a case of continuous and interrupted hard turning, J. Mater. Process. Technol. 170 (2005) 341–349.
[7] Y. Matsumoto, F. Hashimoto, G. Lahoti, Surface integrity generated by precision hard turning, CIRP Ann.-Manuf. Techn. 48 (1999) 59–62.
[8] C. Rao, D. Rao, P. Srihari, Influence of cutting parameters on cutting force and surface finish in turning operation, Procedia Eng. 64 (2013) 1405–1415.
[9] C. Ni, L. Zhu, Z. Zheng, J. Zhang, Y. Yang, R. Hong, Y. Bai, W.F. Lu, H. Wang, Effects of machining surface and laser beam scanning strategy on machinability of selective laser melted Ti6Al4V alloy in milling, Mater. Des. (2020)https://doi.org/10.1016/j.matdes.2020.108880.
[10] D. Xu, Z. Liao, D. Axinte, J.A. Sarasua, R. M'Saoubi, A. Wretland, Investigation of surface integrity in laser-assisted machining of nickel-based superalloy, Mater. Des. (2020)https://doi.org/10.1016/j.matdes.2020.108851.
[11] J. Guo, M. Goh, Z. Zhu, X. Lee, M.L.S. Nai, J. Wei, On the machining of selective laser melting CoCrFeMnNi, Mater. Des. 153 (2020) 211–220.
[12] T. Özel, Y. Karpat, L. Figueira, J.P. Davim, Modelling of surface finish and tool flank wear in turning of AISI D2 steel with ceramic wiper inserts, J. Mater. Process. Technol. 189 (2007) 192–198.
[13] D. Philip Selvaraj, P. Chandramohan, M. Moharanraj, Optimization of surface roughness, cutting force and tool wear of nitrogen alloyed duplex stainless steel in a dry turning process using Taguchi method, Measurement 49 (2014) 205–215.
[14] S.S. Bosheh, P.T. Mativenga, White layer formation in hard turning of H13 tool steel at high cutting speeds using CBN tooling, Int. J. Mach. Tools Manuf. 46 (2006) 225–233.
[15] T. Dawson, T. Kurfess, Tool life, wear rates and surface quality in hard turning, Trans. N. Am. Manuf. Res. Inst. SME (2001) 175–182.
[16] W. Chen, Cutting forces and surface finish when machining medium hardness steel using CBN tools, Int. J. Mach. Tools Manuf. 40 (2000) 455–466.
[17] M. Hasegawa, M. Seireg, R. Lindberg, Surface roughness model for turning, Tribol. Int. 9 (1976) 285–289.
[18] Q. Anq, C. Wang, J. Xu, P. Liu, M. Chen, Experimental investigation on hard milling of high strength steel using PVD-AlTiN coated cemented carbide tool, Int. J. Refract. Met. H. 43 (2014) 94–101.
[19] Y.K. Chou, H. Song, Tool nose radius effects on finish hard turning, J. Mater. Process. Technol. 148 (2004) 259–268.
[20] W. Grzesik, T. Wanat, Surface finish generated in hard turning of quenched alloy steel parts using conventional and wiper ceramic inserts, Int. J. Mach. Tools Manuf. 46 (2006) 1988–1995.
[21] O. Hatt, On the mechanism of tool crater wear in titanium alloy machining, PhD thesis University of Sheffield, Sheffield, 2016.
[22] Sandvik Coromant, How to choose the correct turning insert, [cited 2020 July]; Available from Sandvik Coromant, 2018https://www.sandvik.coromant.com/en-gb/knowledge/general-turning/pages/how-to-choose-correct-turning-insert.aspx.
[23] F. Kara, B. Öztürk, Comparison and optimization of PVD and CVD method on surface roughness and flank wear in hard-machining of DIN 1.2738 mold steel, Sens. Rev. 39 (1) (2019) 24–33.
[24] W.S. Yip, To, S, H.T. Zhou, Social network analysis for optimal machining conditions in ultra-precision manufacturing, J. Manuf. Syst. 56 (2020) 93–103.
[25] AFNOR, *NF E 66–520-4, Norme Francaise. Couple Outil-Matiere (COM) Principle (Turning). ISSN 0335–3931.* 1997.
[26] X.-S. Yang, Optimization Techniques and Applications with Examples, Seventh ed. John Wiley & Sons, Inc., New Jersey, USA, 2018.
[27] A.M. Khan, M.K. Gupta, H. Hegab, M. Jamil, M. Mia, N. He, Q. Song, Z. Liu, C.I. Pruncu, Energy-based cost integrated modelling and sustainability assessment of Al-GnP hybrid nanofluid assisted turning of AISI52100 steel, J. Clean. Prod. (2020) **257**, https://doi.org/10.1016/j.jclepro.2020.120502.
[28] S. Kalpakjian, S. Schmid, Manufacturing Engineering and Technology, Seventh ed. Prentice Hall, New Jersey, USA, 2014.
[29] ISO, STN ISO 3685, Tool-life testing with single-point turning tools, 1999.
[30] C.M. Taylor, I. Cook, R. Alegre, P. Arrazola, P. Spiers, Tool Damage and Adhesion Effects in Turning and Drilling of Hardened Steels, WASET Advanced Manufacturing Technology Conference 2016, pp. 1375–1380.
[31] F. Kara, M. Karabatak, M. Ayyıldız, E. Nas, Effect of machinability, microstructure and hardness of deep cryogenic treatment in hard turning of AISI D2 steel with ceramic cutting, J. Mater. Res. Technol. **9** (**1**) (2020) 969–983.
[32] L. Eriksson, E. Johansson, N. Kettaneh-Wold, C. Wikström, S. Wold, Design of Experiments: Principles and Applications (Third Edition), Umetrics AB, Sweden, 2016.
[33] M. Brown, D. Wright, R. M'Saoubi, J. McGourlay, M. Wallis, A. Mantle, P. Crawforth, H. Ghadbeigi, Destructive and non-destructive testing methods for characterization and detection of machining-induced white layer: a review paper, CIRP J. Manuf. Sci. Tech. 23 (2018) 39–53.
[34] A.K. Saxena, A. Kumar, M. Herbig, S. Brinckmann, G. Dehm, C. Kirchlechner, Micro fracture investigations of white etching layers, Mater. Des. (2019) **180**, https://doi.org/10.1016/j.matdes.2019.107892.
[35] J.P. Davim, Surface Integrity in Machining, Springer, London, 2010.